Fizika Nizkikh Temperatur, 2002, v. 28, No. 7, p. 739–744

Optical study of 4*f* excitations in rare earth cuprates

V. Nekvasil

Institute of Physics, Czech Academy of Sciences, Cukrovarnická 10, 162 53 Prague 6, Czech Republic
E-mail: nekvasil@fzu.cz

Received February 2, 2002

Several recent examples are used to demonstrate that Raman and infrared spectroscopy can be successfully used as a novel experimental tool to study microscopic processes involving 4*f* electrons in rare earth (RE) cuprates. Raman-active crystal field (CF) excitations in Nd_2CuO_4 were measured under hydrostatic pressure up to ~ 7 GPa. The observed pressure-induced shifts of the CF levels were interpreted using density-functional-theory-based *ab initio* calculations and the superposition model. An infrared transmission study of the ${}^4I_J$, $J = 9/2$, $11/2$, $13/2$ multiplets of Nd^{3+} in Nd_2CuO_4 reveals a splitting of the Kramers doublets of the order of a few cm^{-1} due to the Nd–Cu exchange interaction. This study shows that these splittings can be described by an effective anisotropic exchange Hamiltonian for the Nd^{3+} ion expressed in terms of spherical tensor operators up to the sixth order. The isotropic term in the exchange Hamiltonian vanishes for symmetry reasons in this case. An analysis of the infrared transmission spectra in $RE_{1+x}Ba_{2-x}Cu_3O_{6+\delta}$ (RE = Nd, Sm) up to ~ 10 000 cm^{-1} indicates that, besides the regular sites, the RE ions also occupy Ba sites, even in the samples with the cation stoichiometry 1-2-3.

PACS: **78.30.–j**, **71.70.–d**

1. Introduction

The presence of magnetic rare earth (RE) ions has no detrimental effect on superconductivity of the high-T_c cuprates. Therefore, the 4*f* states in RE cuprates have been widely used as a noninteracting probe for examination of superconductivity-related phenomena, including the doping-induced charge transfer from the charge reservoir to the «superconducting» CuO_2 planes, the phase-separation-related charge inhomogeneities and local structure deformations, and the pseudogap openings (for recent surveys see Refs. 1,2). The RE subsystem also exhibits interesting magnetic properties, including strongly anisotropic magnetic moments, Ising-like antiferromagnetism, magnetostriction, or carrier-concentration-dependent spin and lattice dimensionality of the magnetic order [3–7].

An important prerequisite for the study of physical properties of the RE cuprates is an understanding of the microscopic interactions involving 4*f* electrons: the crystal field (CF) interaction, the magnetic exchange interaction, and the coupling of 4*f* excitations and phonons. The principal experimental tool for examining these interactions, by measurements of the 4*f* excitation spectra, has been inelastic neutron scattering [1,2]. Despite the widespread belief that optical methods are not appropriate in opaque materials, sharp and well-resolved 4*f* excitations in RE cuprates have been revealed by infrared (IR) [8] and Raman [9] spectroscopies. Surveyed in this article are recent results illustrating how these two techniques have been used to study microscopic processes involving 4*f* electrons in RE cuprates.

This article is organized as follows. The effect of hydrostatic pressure on the Raman active 4*f* state excitations in Nd_2CuO_4 is studied in the next Section. The splitting of the Kramers doublets in this compound, revealed using the IR spectroscopy, are described in terms of the anisotropic Nd–Cu exchange Hamiltonian in Sec. 3. The 4*f* excitations spectra in $REBa_2Cu_3O_{6+\delta}$ (RE = Nd, Sm) are discussed in Sec. 4.

2. 4*f* spectra in Nd_2CuO_4 under pressure

An interaction with the crystal field produced by the neighboring core charges and valence electronic density is the strongest perturbation of the free ion 4*f*-shell state of trivalent RE ions in cuprates. The CF interaction Hamiltonian is usually considered in the form [10]:

$$H_{CF} = \sum_{k,q} B_{kq} (C_q^{[k]} + C_{-q}^{[k]}), \qquad (1)$$

where the functions $C_q^{[k]}$ transform as tensor operators under simultaneous rotation of the coordinates of all the *f* electrons, B_{kq} are the so-called CF parameters.

The above-mentioned optical methods have made possible the determination of a sufficient number of CF energy levels in Nd_2CuO_4 to ensure reliability of the phenomenological parameters B_{kq} calculated by solving numerically the *inverse secular problem* [9,11].

Recently, CF excitations of the Nd^{3+} ions in Nd_2CuO_4 were measured under hydrostatic pressure using Raman spectroscopy [12]. Two relatively intense CF peaks near 750 cm^{-1} and 1995 cm^{-1} were detected in applied pressure up to ~ 7 GPa. The energy of the 750 cm^{-1} CF excitation within the ground state *J* multiplet increases nearly linearly as a function of pressure at an average rate of 12.9(5) cm^{-1}/GPa (Fig. 1). It shows much larger pressure dependence than the transitions at 1992/1997 cm^{-1} from the ground state to the exchange-split Kramers doublet within the first excited *J* multiplet (Fig. 2). The energies of this

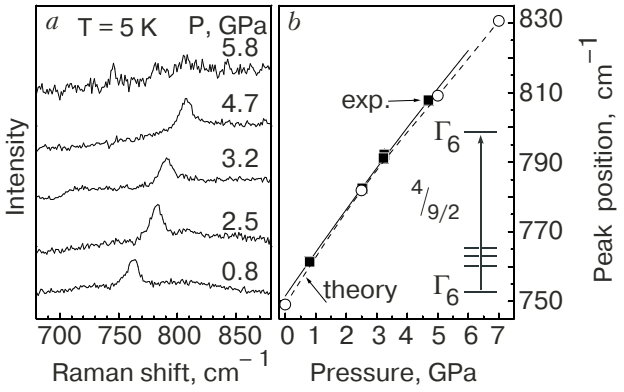

Fig. 1. (*a*) Raman spectra of Nd_2CuO_4 in the spectral range of the 750-cm^{-1} CF excitation for pressures of 0.8–5.8 GPa (T = 5 K). (*b*) Experimental (■, solid line) and calculated (○, dashed line) pressure dependences of the peak position of the CF excitation. The lines in (*b*) are guides to the eye [12].

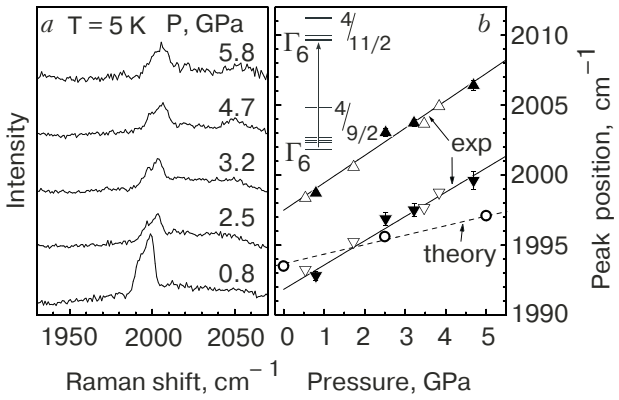

Fig. 2. (a) Raman spectra of Nd_2CuO_4 in the spectral range of the 1995-cm^{-1} CF excitation for pressures of 0.8–5.8 GPa (T = 5 K). (*b*) Experimental and calculated pressure dependences of the peak positions of the CF excitations. The filled and unfilled triangles represent peak positions measured at 5 and 44 K, respectively. The lines represent linear regressions of the data [12].

doublet increase at rates of 1.7(2) cm^{-1} and 2.0(2) cm^{-1}/GPa.

Two theoretical methods were used to interpret the pressure dependence of the CF interaction. The k = 4 and 6 CF parameters were predicted using the superposition model [13] that has proved to be efficient in the CF modeling in cuprates [4]. The model makes it possible to describe the parameters B_{kq} in Eq. (2) in terms of intrinsic (pair) CF parameters $b_k(R)$:

$$B_{kq} = \sum_i S_{kq}(i)\, b_k(R_i), \qquad (2)$$

where $S_{kq}(i)$ is the geometrical factor determined by the angular coordinates of the ligands at the same distance R_i from the RE ion.

The superposition model does not apply to the k = 2 parameters, where the long-range electrostatic contribution dominates. Therefore, the CF parameter B_{20} was calculated using the *ab initio* method, in which the electronic structure and related distribution of the ground state charge density are obtained from calculations based on the density functional theory (DFT). Within the DFT, the CF parameter B_{20}, originating from the effective potential V inside the crystal, can be written as [14]:

$$B_{20} = a_2^0 \int_0^\infty |R_{4f}(r)|^2 V_2^0(r) r^2 dr, \qquad (3)$$

where nonspherical components $V_2^0(r)$ reflect not only the nuclear potentials and Hartree part of the inter-electronic interaction but also the exchange correlation term, which accounts for many-particle

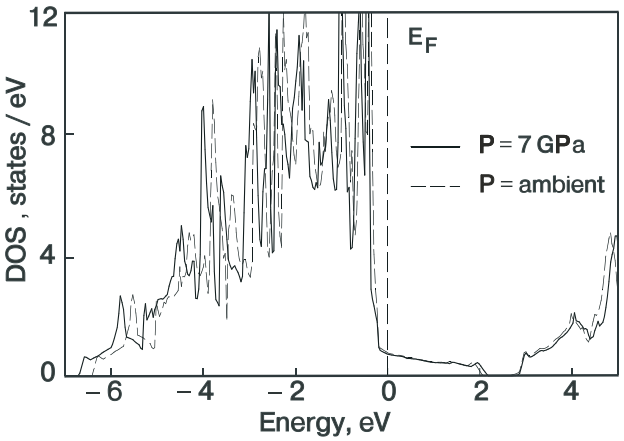

Fig. 3. Total density of electron states (DOS) of Nd_2CuO_4 calculated at ambient pressure and at 7 GPa [12].

effects. The radial wave function R_{4f} describes the radial shape of the localized $4f$ charge density of the RE^{3+} ion in the compound studied.

The calculation of the pressure dependence of the CF parameters included two steps. First, Eqs. (2), (3) were used to calculate the theoretical ratio $B_{kq}(P)/B_{kq}(0)$ with allowance for the data on the pressure evolution of the Nd_2CuO_4 crystal structure measured by synchrotron x-ray powder diffraction [15] and the available superposition model parameters [4]. The effect of pressure on the underlying electronic density of states (DOS) is shown in Fig. 3. It is worth noting that the DOS curve is broadened by ~ 0.5 eV at an applied pressure of 7 GPa. This broadening is connected with a slight redistribution of the charge density, which results in an increase of the absolute value of the calculated parameter B_{20} . In the second step each phenomenological parameter B_{kq} [11] was multiplied by the theoretical ratio $B_{kq}(P)/B_{kq}(0)$. As an illustration, the CF parameters obtained in this way for the applied pressure 7 GPa are compared with the ambient pressure parameters in Table 1. The absolute values of the individual CF parameters are increased by ~ 6–18 % at 7 GPa compared to those at zero pressure.

Table 1

CF parameters B_{kq} in Nd_2CuO_4 (in cm^{-1}) obtained from a fit to IR absorption data at ambient pressure [11] and calculated at 7 GPa using the superposition model and the DFT based *ab initio* method (see text)

Parameter	$P = 0$ [11]	$P = 7$ GPa [12]
B_{20}	−335	−373
B_{40}	−2219	−2574
B_{44}	1634	1935
B_{60}	224	246
B_{64}	1494	1584

The theoretical approach described above gives transition frequencies increasing nearly linearly at rates of ~ 11.7 and ~ 0.7 cm^{-1}/GPa for excitations near 750 and 1992(1997) cm^{-1}, respectively. Regarding the lower-energy transition, very good agreement is achieved with the experimental result of 12.9 cm^{-1} (Fig. 1). The calculated value of the pressure dependence of the higher energy transitions is smaller than the experimental values of ~ 1.7 and 2.0 cm^{-1} for the peaks at 1992 and 1997 cm^{-1} (Fig. 2), respectively. It bears noting that these transitions include the ground-state level and the lowest energy level in the $J = 11/2$ multiplet. The CF calculation shows that the pressure dependences of these levels are very similar, −4.5 and −3.8 cm^{-1}/GPa, respectively. This explains why the resulting pressure-induced shift of the transition energy is small. The remaining discrepancy between the experimental and calculated values is ascribed to a small pressure-induced shift of the free ion levels, not taken into account in the above calculations.

A detailed analysis of the pressure-induced increase in the separation of the doublet near 1995 cm^{-1} (Fig. 2) indicated that in addition to the CF parameters the parameters α_{kq} of the Hamiltonian of the anisotropic Nd–Cu exchange interaction, Eq. (4), are pressure dependent [12].

3. Anisotropy of the Nd–Cu exchange interaction in RE cuprates

The IR transmission study of the $4f$ spectra in the antiferromagnet Nd_2CuO_4 yielded a splitting of the CF Kramers doublets of the order of a few cm^{-1} due to the exchange interaction between Nd and Cu (see the third column of Table 2) [16]. An example of the experimental spectra of the transition from the ground state to an exchange-split Kramers doublet at ~ 5870 cm^{-1} is shown in Fig. 4. The exchange anisotropy due to the orbital moments of the f electrons is pronounced in this case: the isotropic Heisenberg-type exchange alone appears to be completely incapable of explaining the observed doublet splittings [11]. To account for these splittings one has to consider the complete Hamiltonian within the molecular field approximation describing the exchange interaction of the $4f$

electrons of an Nd ion with the magnetically polarized Cu sublattice [17,18].

Table 2

Splitting of the Nd^{3+} Kramers doublets in Nd_2CuO_4 as measured by infrared transmission [16] and calculated using Eq. (4) [19] (all energies in cm^{-1})

J multiplet	CF level [10]	Observed splitting	Calculated splitting
9/2	Ground state	5.5	5.7
11/2	1995	3.5	3.7
	2006	3.5	3.5
	2013	4.0	3.7
	2077	2.0	2.1
	2414	3.0	2.9
13/2	3950	2.5	2.7
15/2	5868	2.0	1.3

The perturbation single-ion Hamiltonian under consideration then includes, besides the standard CF term H_{CF} from Eq. (1), an exchange term H_{exch}:

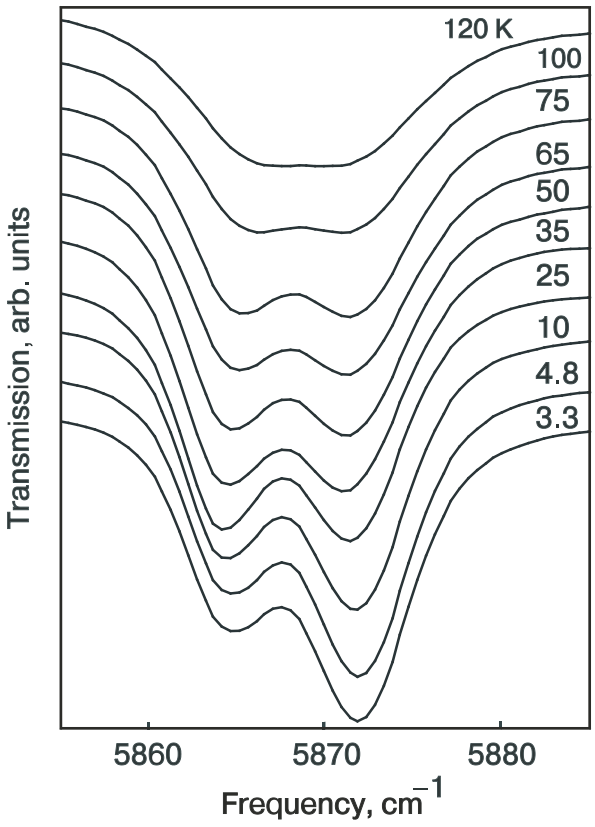

Fig. 4. Nd_2CuO_4 IR transmission as a function of temperature [16].

$$H_{\text{exch}} = -2\sum_{k,q} \alpha_{kq} \sum_i T_q^{[k]}(i)\mathbf{s}(i)\cdot\mathbf{n}, \qquad (4)$$

where α_{kq} are the exchange parameters, $T^{[k]}(i)$ are the irreducible unit tensor operators which act on the orbital part of the Nd wave function, $\mathbf{s}(i)$ is the spin of a Nd electron, and $\mathbf{n}$ is the unit vector directed along the magnetization of the Cu sublattice. There are six independent parameters α_{kq} in H_{exch} for Nd ions occupying the tetragonal symmetry sites in Nd_2CuO_4.

A least-squares procedure has been utilized to fit the splitting of the eight observed Kramers doublet splittings using the above-mentioned perturbation Hamiltonian [19]. The results of the final fit are summarized in Table 2; the corresponding best-fit values of α_{kq} are given in Table 3. It is worthwhile to note that the contributions of the second- and fourth-order terms to the splittings are two orders of magnitude larger than that of the isotropic term ($k = q = 0$) in the exchange operator. This finding is compatible with the symmetry considerations indicating that the isotropic term in the exchange Hamiltonian vanishes when only the nearest Cu neighbors of Nd are considered [20]. It also shows the importance of the higher-order terms in Eq. (4), neglected in magnetic studies in which the anisotropic RE–Cu coupling in Nd_2CuO_4 [20,21] and $PrBa_2Cu_3O_{6+\delta}$ [22,23] is represented by a pseudo-dipolar term.

Table 3

The best-fit values of the exchange parameters α_{kq} (in cm^{-1}) in Eq. (4) [19]

Exchange parameter α_{kq}	
α_{00}	−7(4)
α_{20}	−491(130)
α_{40}	−177(33)
α_{44}	−257(12)
α_{60}	15(16)
α_{64}	47(13)

4. Crystal field study in $RE_{1+x}Ba_{2-x}Cu_3O_{6+\delta}$ (RE = Nd, Sm)

In this Section we report a systematic study of CF transitions in $NdBa_2Cu_3O_{6+\delta}$ ($\delta \sim 0$) and $Sm_{1+x}Ba_{2-x}Cu_3O_{6+\delta}$ ($x \leq 0.01$, $x = 0.03$, 0.05, and 0.11; $\delta \sim 0$) by IR absorption [24,25]. The transitions involving Kramers doublets within the low-

est-energy ^4I term and ^6H term in the Nd and Sm compounds, respectively, were determined. Examples of these transitions are shown in Figs. 5 and 6. The large number of peaks in the experimental spectra indicates that there exists more than one type of RE site. We observe that the *f–f* transitions are electric-dipole forbidden for the RE ions at regular D_{4h}-symmetry sites in ideal $REBa_2Cu_3O_6$.

A phenomenological CF analysis of the IR data (Sec. 2), including the neutron scattering data for the $J = 9/2$ multiplet in $NdBa_2Cu_3O_6$ [26], allowed identification and fitting of the CF spectra of Nd and Sm ions at regular sites. Detailed CF calculations using the superposition model and the *ab initio* method based on the density-functional theory described in Sec. 2 indicate [27] that additional bands in the IR spectra correspond to the RE^{3+} ions in the C_{4v}-symmetry Ba sites. The sets of the CF parameters for regular as well as Ba sites obtained using the above-mentioned methods are summarized in Table 4.

Concluding this part, we note that the CF transitions at RE/Ba sites have been observed in all $RE_{1+x}Ba_{2-x}Cu_3O_{6+\delta}$ samples studied, including

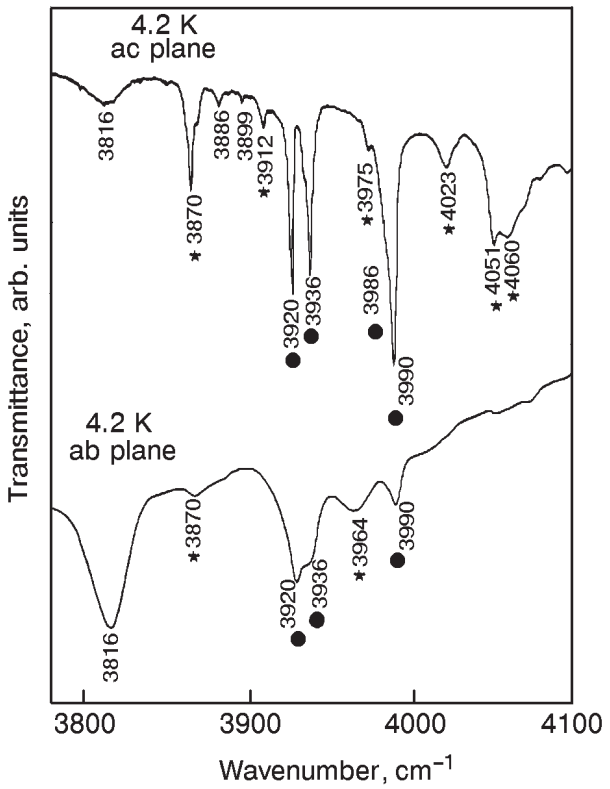

Fig. 5. IR spectra of CF transitions in $NdBa_2Cu_3O_6$ from the ground state multiplet $^4I_{9/2}$ to the second excited multiplet $^4I_{13/2}$ (*ab* and *ac* platelets at 4.2 K). The filled circles and asterisks indicate strong and weak absorption bands, respectively. See Ref. 24 for additional details.

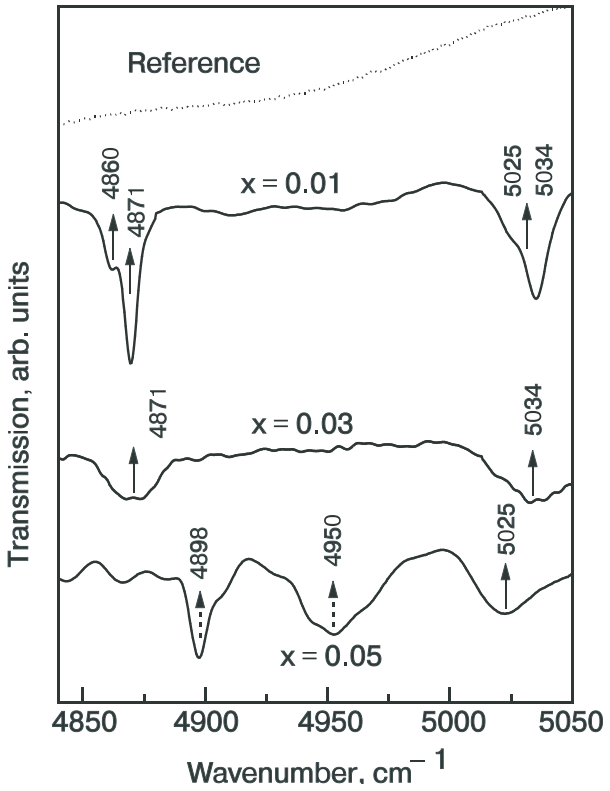

Fig. 6. IR spectra of CF transitions ($^6H_{5/2} \rightarrow {}^6H_{13/2}$) in $Sm_{1+x}Ba_{2-x}Cu_3O_{6+\delta}$ in the 4800–5050 cm^{-1} range. The dashed arrows indicate CF transitions associated with Sm/Ba sites. See Ref. 25 for additional details.

those with $x = 0$. This finding supports recent data indicating that the presence of a relatively small quantity of the magnetic Pr^{3+} ions at the Ba sites is the main reason for anomalous behavior of $PrBa_2Cu_3O_7$, including the suppression of superconductivity as well as the appearance of the antiferromagnetic ordering in the Pr sublattice at a

Table 4

CF parameters (in cm^{-1}) in $Sm_{1+x}Ba_{2-x}Cu_3O_6$ [6] and $Nd_{1+x}Ba_{2-x}Cu_3O_6$ [5] obtained by an analysis of the IR spectra (see text)

B_{kq}	D_{4h} site		C_{4v} site
$k\ q$	Sm	Nd	Sm
2 0	282(5)	380(28)	−227
4 0	−2481(12)	−2956(34)	24
4 4	1307(10)	1664(25)	−331
6 0	321(12)	526(15)	−427
6 4	1931(6)	2021(10)	624

temperature at least one order of magnitude higher than for other RE elements [28].

Acknowledgements

The assistance of the Grant Agency of the Czech Republic in the form of its grant No. 202/00/1602 is gratefully acknowledged.

1. U. Staub and L. Soderholm, in: *Handbook on the Physics and Chemistry of Rare Earth,* Vol. 30, K. A. Gschneidner, Jr., L. Eyering, and M. B. Maple (eds.), North Holland, Amsterdam (2001), p. 491.
2. J. Mesot and A. Furrer, *J. Supercond.* **10,** 623 (1997).
3. T. W. Clinton and J. W. Lynn, *Phys. Rev.* B**51,** 15429 (1995).
4. V. Nekvasil, *J. Magn. Magn. Mater.* **140–144,** 1265 (1995); Nekvasil, M. Divis, G. Hilscher, and E. Holland-Moritz, *J. Alloys Comps.* **225,** 578 (1995).
5. V. Nekvasil, S. Jandl, T. Strach, T. Ruf, and M. Cardona, *J. Magn. Magn. Mater.* **177–181,** 535 (1998).
6. I. K. Aminov, B. Z. Malkin, and M. A. Teplov, in: *Handbook on the Physics and Chemistry of Rare Earth*, Vol. 22, K. A. Schneider, Jr. and L. Eyering, (eds.), North-Holland, Amsterdam (1996), p. 295.
7. V. V. Eremenko, T. V. Sukhareva, and V. N. Samovarov, *Phys. Solid State* **42,** 816 (2000).
8. M. L. Jones, D. W. Shortt, B. W. Sterling, A. L. Schawlow, and R. M. Macfarlane, *Phys. Rev.* B**46,** 611 (1992).
9. S. Jandl, M. Iliev, C. Thomsen, M. Cardona, B. M. Wanklyn, and C. Changkang, *Solid State Commun.* **87**, 609 (1993); S. Jandl, P. Dufour, T. Strach, T. Ruf, M. Cardona, V. Nekvasil, C. Chen, and B. M. Wanklyn, *Phys. Rev.* **B52,** 15558 (1995).
10. B. G. Wybourne, S*pectroscopic Properties of Rare Earths,* Wiley, New York (1965).
11. S. Jandl, P. Dufour, P. Richard, V. Nekvasil, D. I. Zhigunov, S. A. Barilo, and S. V. Shiryaev, *J. Lumin.* **78,** 197 (1998).
12. I. Loa, K. Syassen, M. Divis, V. Nekvasil, S. Jandl, A. A. Nugroho, and A. A. Menovsky, *Phys. Rev.* **B64,** 214106 (2001).
13. D. J. Newman and Betty Ng, *Rep. Prog. Phys.* **52,** 699 **(1989)**.
14. M. Divis, V. Nekvasil, and J. Kuriplach, *Physica* **C301,** 23 (2998); M. Divis and V. Nekvasil, *J. Alloys Comps.* **323–324,** 567 (2001).
15. H. Wilhelm, C. Cross, E. Reny, G. Demazeau, and M. Hanfland, *J. Mater. Chem.* **8,** 2729 (1998).
16. S. Jandl, P. Richard, V. Nekvasil, D. I. Zhigunov, S. N. Barilo, and S. V. Shiryaev, *Physica* **C314** 189 (1999).
17. P. M. Levy, *Phys. Rev.* **135**, 155 (1964).
18. W. P. Wolf, *J. Phys. (Paris)* **32**, C1–26 (1971).
19. A. A. Nugroho, V. Nekvasil, I. Veltrusky, S. Jandl, P. Richard, A. A. Menovsky, F. R. de Boer, and J. J. M. Franse, *J. Magn. Magn. Mater.* **226–230,** 973 (2001).
20. R. Sachidanandam, T. Yilidirim, A. B. Harris, A. Aharony, and O. Entin-Wohlman, *Phys. Rev.* B**56,** 260 (1997).
21. Ph. Bourges, L. Boudarene, and D. Petitgrand, *Physica* **B180–181,** 128 (1992).
22. S. V. Maleev, *JETP Lett.* **67,** 947 (1998).
23. S. J. S. Lister, A. T. Boothroyd, N. H. Andersen, B. H. Larsen, A. A. Zhokhov, A. N. Christensen, and A. R. Wildes, *Phys. Rev. Lett.* **86,** 5994 (2001).
24. A. A. Martin, T. Ruf, M. Cardona, S. Jandl, D. Barba, V. Nekvasil, M. Divis, and T. Wolf, *Phys. Rev.* **B59,** 6528 (999).
25. D. Barba, S. Jandl, V. Nekvasil, M. Marysko, M. Divis, T. Wolf, A. A. Martin, C. T. Lin, and M. Cardona, *Phys. Rev.* **B63,** 54528 (2001).
26. P. Allenspach, J. Mesot, U. Staub, M. Guillaume, A. Furrer, S.-I. Yoo, M. J. Kramer, R. W. McCallum, H. Maletta, H. Blank, H. Mutka, R. Osborn, M. Arai, Z. Bowden, and A. D. Taylor, *Z. Phys.* **B95**, 301 (1995).
27. M. Divis and V. Nekvasil, *J. Alloys Comps.* **323–324,** 567 (2001).
28. H. A. Blackstead, J. D. Dow, I. Felner, and W. B. Yelon, *Phys. Rev.* **B63,** 094517 (2001).